Net-like Assembly of Au Nanoparticles as a Highly Active Substrate for Surface-Enhanced Raman and Infrared Spectroscopy

Zhixun Luo,[†,‡] Wensheng Yang,[§] Aidong Peng,[†] Ying Ma,[†] Hongbing Fu,[†] and Jiannian Yao*[,†]

Beijing National Laboratory for Molecular Science (BNLMS), Institute of Chemistry, Chinese Academy of Sciences, Beijing 100190, People's Republic of China, Graduate School of the Chinese Academy of Sciences, Beijing, 100049, People's Republic of China, and College of Chemistry, Jilin University, Changchun 130012, People's Republic of China

Received: November 26, 2008; Revised Manuscript Received: January 14, 2009

Anodic aluminum oxide (AAO) templates were employed to filtrate and assemble Au nanoparticles by the pressure difference method. It was found that the colloidal Au nanoparticles can be uniformly arranged as nanonet assembly on the AAO surface. The net-assembled Au nanoparticles are clean and closely packed with nanochains. Taking fullerene C_{60}/C_{70} as probe molecules, high-quality surface-enhanced Raman scattering (SERS) spectra were observed. The net-assembled Au nanoparticles even synchronously support the observation of surface-enhanced infrared absorption (SEIRA) spectra of the fullerene C_{60}/C_{70}. These results indicate that the AAO template filtrated with net-assembled Au nanoparticles is a highly active substrate for surface-enhanced spectroscopy.

1. Introduction

Optical properties of noble metal nanoparticles have drawn particular interest due to their significant applications as optical filters,[1] bio/chemosensors,[2] plasmonic waveguides,[3] and as active substrates for surface enhanced spectroscopy.[4] The unique optical properties of noble metal nanoparticles primarily originate from the localized surface plasmon resonance (LSPR), which is a collective oscillation of the conduction electrons that occur when light with a specific wavelength impinges on a noble metal nanoparticle. The LSPR is dependent on the size, shape, composition,[5] and dielectric character of the nanoparticle,[6] and is usually documented as surface-enhanced Raman scattering (SERS), as well as surface-enhanced Infrared absorption (SEIRA).[7]

To improve the LSPR effect, recently adjacent nanoparticles and their optical properties on SERS and SEIRA have been explored by many research groups.[8] Van Duyne and co-workers studied short-range coupling effects in hexagonal and square arrays of triangular and cylindrical gold and silver nanoparticles[9] and the plasmon resonance of a finite 1D chain of the nanoparticles.[10] Zhang and co-workers[11] studied the 1D chain of gold nanoparticles experimentally and theoretically, and they observed nonmonotonic behavior of the plasmon resonance shift for the condition where the phase retardation effect affects the resonance wavelength. However, most of these arrays of the nanoparticles were achieved by physical lithography, which differs from large area self-assembly, and shows limitations to their applications in miniaturized devices, sensors, and high-density data storage.[12] Vaporization-induced self-assembly has also been developed and emerged as an elegant "bottom up" method for assembly of the nanoparticles.[13,14] Recently Cai and co-workers reported the spontaneous formation of ordered patterns of nanoparticles by the Marangoni flow of ethanol into water, called the "tears of wine" phenomenon.[15] Despite these findings, it is still a challenge to assemble nanoparticles in desired locations exhibiting ordered patterns via a simple process.

The ordered AAO template has been reported as a versatile approach for nanorods, nanotubes, and many other one-dimensional materials and arrays.[16−21] Despite this progress, there have been few reports on the application of the AAO as a substrate for controlling the assembly of nanoparticles on its surface. In this work, we employ the AAO template to act as a nanosieve for the filtration and assembly of Au nanoparticles. It was found that colloidal Au nanoparticles can be arranged as nanonet assembly via the pressure difference method. The net-assembled Au nanoparticles present a rather different SERS spectra of fullerene C_{60} and C_{70} as from other substrates and even sharply differ from the monolayer of the Au nanoparticles coated on the same AAO templates. Furthermore, the net-assembled Au nanoparticles also present obvious SEIRA activity. It is shown that the AAO template filtrated with net-assembled Au nanoparticles is a highly SERS active substrate and also a good sublayer for SEIRA.

2. Experimental Section

All chemicals used are of reagent grade unless otherwise specified.

Au colloid was prepared through a redox process based on Frens's method,[22] except that $KAuCl_4$ was used instead of $HAuCl_4$. A 75 mg sample of $KAuCl_4$ was dissolved in 500 mL of deionized water and the solution was heated to boiling. Then 10 mL of sodium citrate aqueous solution (87.87 mg of sodium citrate in 10 mL of deionized water) was added into the boiling $KAuCl_4$ solution dropwise, accompanied by vigorously stirring. The mixed solution was kept boiling for a further 10 min.

The AAO templates were prepared according to a method described previously.[16] Before anodizing, aluminum foils (99.999% purity, Institute of Nonferrous Metal, Chinese Academy of Sciences) were first degreased in acetone and then annealed at 350 °C for 2 h. The annealed aluminum foils were

* Corresponding author.
[†] Beijing National Laboratory for Molecular Science (BNLMS), Institute of Chemistry, Chinese Academy of Sciences.
[‡] Graduate School of the Chinese Academy of Sciences.
[§] College of Chemistry, Jilin University.

10.1021/jp810387w CCC: $40.75
Published on Web 02/13/2009

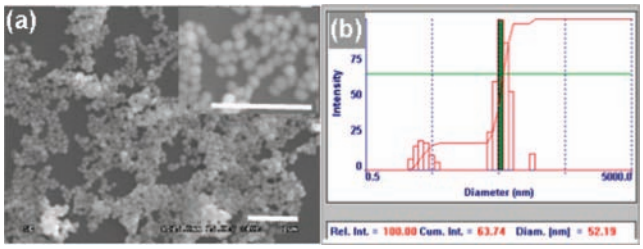

Figure 1. SEM characters of the colloidal Au nanoparticles on a silicon piece (a) and its dimension distribution measured by DLS (b).

etched in a mixture of perchloric acid and ethanol (1:4) for several minutes and then anodized at a constant voltage (ca. 20−80 V) in oxalic acid (ca. 0.4−0.6 M) at 10 °C for 2 h. The surface alumina layer formed was removed in a mixture of phosphoric acid (6 wt %) and chromic acid (1.5 wt %), and the aluminum foils were reanodized at the same conditions as before for 2.5 h. A honeycomb structure of anodic porous alumina was then obtained. The as-prepared alumina membrane has an average thickness of 20−80 μm. The pores of the template were uniformly arranged in a close-packed hexagonal lattice, and they were continuous and parallel to one another. The diameter of the pores could be varied between 20 and 200 nm by controlling the experimental conditions.

One of these complete AAO templates was placed into a Buchner funnel with a fritted disk (G4) that connected to an accessory flask with a sidearm, keeping the vacuum production, then the Au colloid was gradually dropped onto the AAO template. After a few minutes rest the procedure was repeated several times before vacuum drying.

C_{60}/C_{70} was dissolved in pyridine by an ultrasonic assisted dissolving method. The concentration of the solutions of C_{60}/C_{70} is 0.01 M for all the experiments. One milliliter of the solution was dropped on the as-prepared substrates and dried completely before they were used as SERS samples. Infrared and Raman spectra were acquired with a FT-Raman and infrared spectrometer. A Brucker Model IFS-66 FT-Raman spectrophotometer with a line resolution of 3 cm^{-1} and a YAG laser (CW) operated at 1064 nm were used as the excitation source at 50 mW. DLS (Dynamic Light Scattering) measurement was performed with a particle size analyzer (BI-90Plus, Brookhaven Instruments) with a scattering angle of 90°. The morphology and size of the samples were examined by field emission scanning electron microscopy (FESEM, Hitachi S-4300). All the SEM samples were adhered with conductive adhesive tape.

3. Results and Discussion

Figure 1a presents the SEM image of the prepared colloidal Au nanoparticles (separated on silicon piece). DLS analysis shows the particle size is uniformly distributed with a dimension of about 52 nm (Figure 1b).

The Au nanoparticles were assembled on porous AAO templates via the pressure differences method. Figure 2 presents the SEM images of the Au nanoparticles supported on different AAO templates with the same quantities of Au colloid added, where parts a and b of Figure 2 refer to the templates with pore dimensions of 200 and 20 nm, respectively. It is noted that the Au nanoparticles can be well organized on the porous AAO templates via the pressure differences. Under the same pressure difference, net-like assembly is formed on the 200 nm AAO templates (Figure 2a) and layer-coating assembly is formed on the 20 nm AAO template (Figure 2b). It should be mentioned that an AAO template with a relatively larger pore dimension

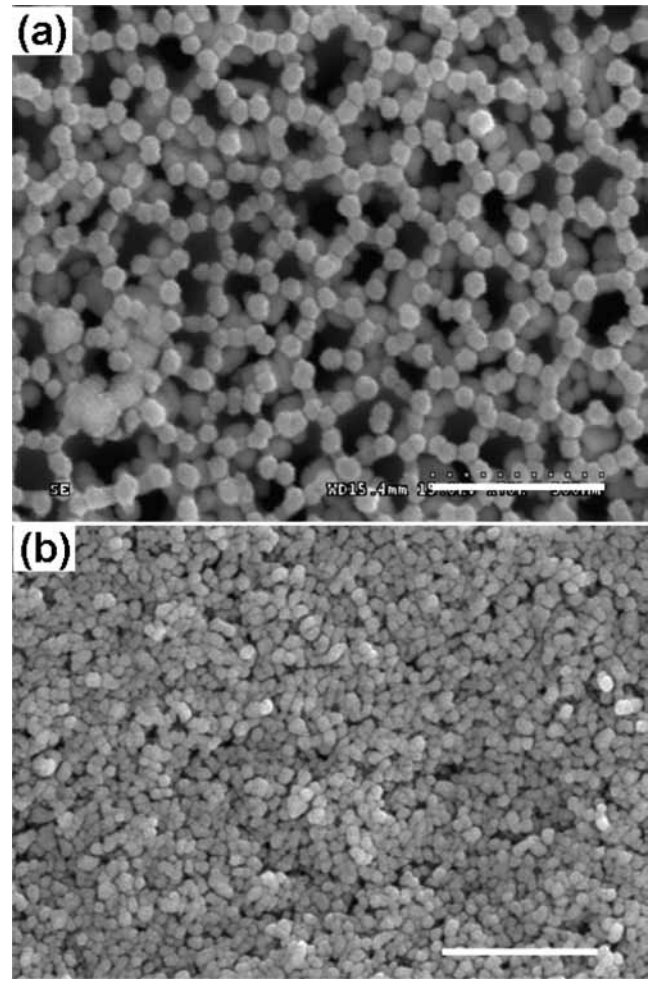

Figure 2. SEM characters of the net-like assembled colloidal Au nanoparticles on 200 nm pores of AAO membrane (a, and particle-coatings on 20 nm pores of alumina membrane (b) viathe pressure difference method: the dimension bar is 500 nm for all.

will allow quantities of the Au nanoparticles to fall into the pores under a certain pressure difference except for opportunities for adhering on the edge of the AAO pores. As a result, the cleaned Au nanoparticles can be realigned and assembled into chains and further be connected into the net-like pattern, which is clearly composed of the corresponding Au nanoparticles.[23]

We first launched the applicability of the net-assembled Au nonoparticles on SERS spectroscopy. Figure 3 shows the measured SERS spectra of fullerene C_{60}. The sphere fullerene C_{60} actually has been employed as probe molecule for SERS by some groups due to its unique properties.[24−27] Figure 3a shows the FT-Raman spectrum of solid C_{60} powder, while Figure 3b gives the SERS spectrum from the net-assembled Au nanoparticles on 200 nm AAO template. The high degeneracy degree in the C_{60} molecule makes the spectrum appear rather simple, in spite of the large number of atoms per molecule. Besides the expected 10 Raman active vibrational modes obviously appearing in correlative bands, an infrared active mode is also observed at 433 cm^{-1}, which may originate from the symmetry lowering by the intermolecular interaction in solid C_{60} (Figure 3a).

The measured SERS spectrum presents rather strong peaks compared with the FT-Raman of solid C_{60} powder (Figure 3b). Raman intensities of all the modes are strongly enhanced, with an estimated enhancement factor up to 10^5 compared with that of pure C_{60} solution, which accords well with the reported SERS

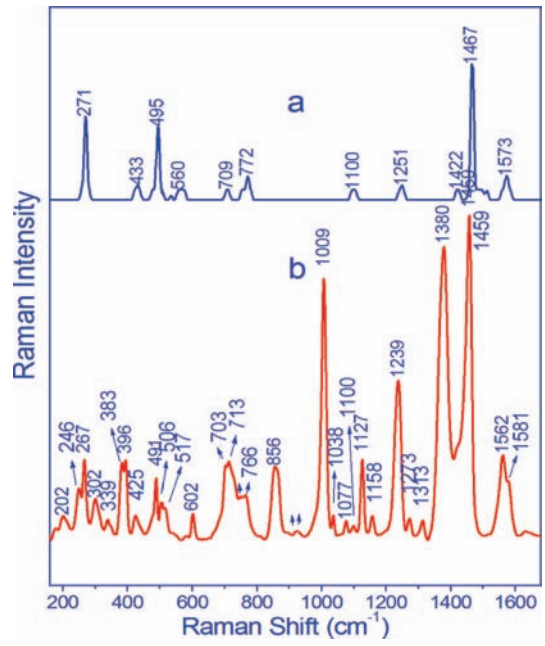

Figure 3. FT-Raman of solid fullerene C_{60} (a) and SERS of C_{60} from the net-assembled Au nanoparticles on an AAO template (b).

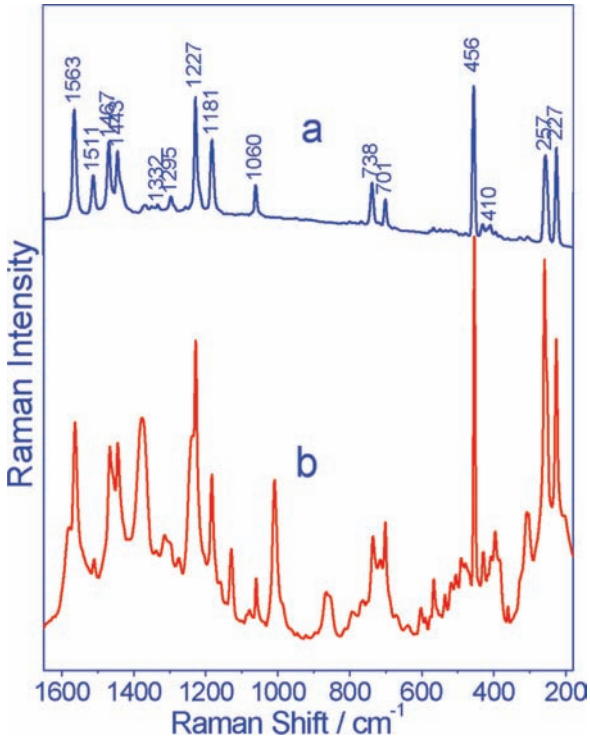

Figure 4. FT-Raman spectrum of solid fullerene C_{70} (a) and SERS spectrum of C_{70} from the net-assembled Au nanoparticles (b).

measurement.[27] However, it presents almost a completely different Raman spectral profile of C_{60}. It is noted that the normally obtained three main strong peaks at 273, 497, and 1467 cm^{-1} in solid C_{60} are not predominant again in the SERS spectrum. Furthermore, not only does the number of vibrational modes increases greatly, but also the Raman bands split as well as the shift of the frequencies (Table 1). The appearance of abundant additional peaks suggests the decrease in degeneracy degree of the energy level, ascribed to the symmetry lowering and selection rule relaxation of C_{60} induced by the gold surface.[25−27]

TABLE 1: Raman Modes of Fullerene C_{60} Obtained and Their Symmetry Assignments

Raman modes of C_{60} (cm^{-1})			
FT-Raman	SERS from colloidal Au monolayer	SERS from colloidal Au nanonet	assignment (symmetry)
497	494	491	Ag (2)
1467	1468	1459	
273	257/270	246/267/302	Hg (8)
433	428	425	
716	703	703/713	
772	770	749/766	
1108	998	1100	
1251	1251	1273	
1430	1427	1426	
1575	1569	1581	
535	535	506/517	T1u (4)
570	570	602	
		1158	
		856	T1g (3)
		1273	
		602	T2g (4)
		713	
		749/765	Gg(6)
	1024	1038/1077	
		1313	
		1009	Au
	1200	1158	T2u(5)
		765	Gu(6)
		1313	
		1239	Hu(7)
		1562	

The lowest unoccupied molecular orbit (LUMO) of fullerene C_{60} is 3-fold degeneracy (T_{1u}), and the highest occupied molecular orbit (HOMO) is 5-fold degeneracy (H_u). Group theory allows 46 vibrations forthe C_{60} molecule ($A_u + 2A_g + 3T_{1\,g} + 4T_{1u} + 4T_{2\,g} + 5F_{2u} + 6G_g + 6G_u + 7H_u + 8H_g$). For I_h symmetry, only the two A_g and eight H_g vibrations are Raman active, and the four F_{1u} modes are infrared active, as well as 22 hyper-Raman active ($4T_{1u} + 5T_{2u} + 6G_u + 7H_u$) modes. Pentagonal adsorption would result in retro-gradation of the C_{60} molecule group from the high symmetric I_h group to the C_{5v} group and hexagonal adsorption from I_h to C_{3v}. Because of this, H_g, T_{1u}, and some other modes of the I_h group would split into two or three modes of C_{3v} and C_{5v} groups with lower degeneracy. Herein, the SERS spectrum of C_{60} from the net-assembly is consistent with these. As the normal coordinate of low-frequency modes is mostly radial along the molecule, the group theory calculation concludes that there are three splits for the H_g mode. It is seen that the Hg modes split as expected from the group theory. For instance, the 273 cm^{-1} mode splits into three independent peaks as observed at 246, 267, and 302 cm^{-1}, and the 433 cm^{-1} mode also splits into three peaks at 425, 383, and 396 cm^{-1}. The split is also observable for the high-frequency H_g mode at 1575 cm^{-1}, which turns into a 1562 cm^{-1} mode with a shoulder at 1581 cm^{-1} in the SERS spectrum.

Compared to those of solid C_{60}, the peaks in the SERS spectrum also experience a little red-shift. For example, the peak at 497 cm^{-1} shifts to 491 cm^{-1}, the one at 1467 cm^{-1} shifts to 1459 cm^{-1}, and the one at 1575 cm^{-1} shifts to 1562 cm^{-1}. It has been known that Au atoms can bind to C_{60} in an argon matrix to form an adduct product, Au−C_{60} complex. The symmetry reduction in this charge transfer complex will allow more vibrational modes to become infrared-active.[24] On the basis of the above discussions, we conclude that the net-assembly of Au nanoparticles led to a more severe symmetry lowering of the adsorbed C_{60} molecules.

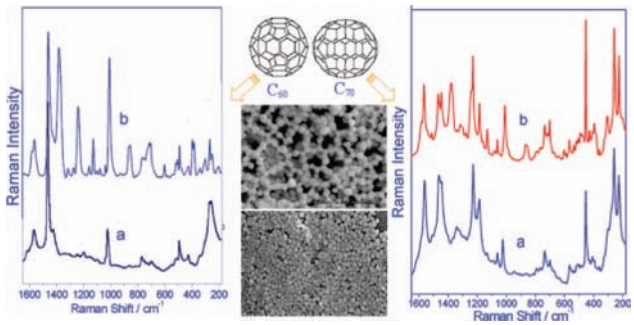

Figure 5. (Left) SERS spectrum of fullerene C_{60} from monolayer-coating of Au nanoparticles (a) compared with that from the net-assembled Au nanoparticles (b). (Right) SERS spectrum of fullerene C_{70} from monolayer-coating of Au nanoparticles (a) compared with that from the net-assembled Au nanoparticles (b).

Similar measurements were also taken for fullerene C_{70} molecules. Figure 4a gives the FT-Raman spectrum of solid fullerene C_{70}, while Figure 4b refers to the SERS spectrum of C_{70} from the net-assembled Au nanoparticles on a 200 nm AAO template. It is noted that Figure 4b obviously shows finer spectral features than the solid Raman spectrum of C_{70}. Many more Raman peaks observed further indicate that the net-assembled Au nanoparticles have better SERS activity than the monolayer coatings for the fullerene molecules. A C_{70} molecule can be viewed to be formed by two semicircular caps of 30 carbon atoms, substantially identical to half the C_{60} cluster, separated by an equatorial belt of 10 atoms. Similar to fullerene C_{60}, a free C_{70} molecule belongs to the D_{5h} symmetry group and the 204 normal vibrations classify as $12A_1 + 9A_2 + 21E_1 + 22E_2 + 9A_1 + 10A_2 + 19E_1 + 20E_2$. The E_1 and A_2 modes are infrared active and the A_1, E_2, and E_1 modes are Raman active.[27]

Because both the C_{60} and C_{70} molecules are spherical or elliptical, the intrinsic oscillating modes, including breathing vibrations, torsional modes and ellipsoid modes, should all belong to low-energy phonon spectra. Among them, the frequencies of torsional modes or ellipsoid modes may be related to the longitudinal or lateral velocity of sound.[27,28] These abundant Raman modes that appeared in correlative bands is ascribed to the high sensitivity of SERS in this system. As we can see from Figure 4b, many sharp and narrow peaks are observed. For example, many small peaks blossom out around the 456 cm^{-1} mode. The classes of foot peaks, shoulder peaks, and brother peaks appeared as a result of molecular symmetry lowering.[24−27]

The measured SERS spectra of fullerene C_{60} and C_{70} from the net-assembled Au nanoparticles not only show the sharp difference from their usual SERS,[24−27] but also differ much from their SERS based on the layer-coating assembly of the same Au nanoparticles on the AAO templates, as shown in Figure 5. It shoudl be mentioned that the SERS spectra from the monolayer coatings of Au nanoparticles on AAO templates present rare difference from those observed from the gold-C_{60}/C_{70} clusters on various substrates. However, it differs very much compared with the SERS from the net-assembled Au nanoparticles. Especially for the C_{60} system, the two SERS spectra present much difference compared with each other, except for a few intrinsic modes. Detailed comparison and assignment are given in Tables 1 and 2, respectively. It is notable that fullerene C_{60} and C_{70} are very stable molecules which cannot form chemical complexation with Au nanoparticles. The appearance of additional and split modes resulted from the different symmetry lowering and selection rule relaxation by the adsorption of C_{60}/C_{70} on the two sorts of Au-coated substrates. In addition, the possible weak interaction (ca. Coulomb force) in the ground state of C_{60}/C_{70} on the net-like assembly with respect to monolayer coatings of Au nanoparticles may also bring forth minor influence to the different SERS observation.

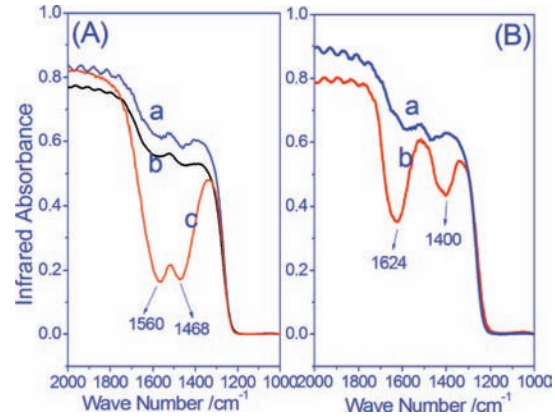

Figure 6. (A) Infrared absorption spectra of only C_{60} on AAO template with pyridine as solvent (a), and only Au nanoparticles on the AAO template (b), and C_{60} on the net-assembled Au nanoparticles-coated AAO template with pyridine as solvent (c). (B) Infrared absorption spectra of only C_{70} on AAO template with pyridine as solvent (a) and C_{70} on Au nanoparticles-coated AAO template with pyridine as solvent (b).

TABLE 2: Raman-Mode of Fullerene C_{70} Obtained and Their Symmetry Assignments

exptl Raman modes of C_{70} (cm^{-1})			
FT-Raman	SERS from colloidal Au monolayer	SERS from colloidal Au nanonet	assignment (symmetry)
225	227	226	E2′
257	259	258	A1′
		309	E2″
	361	395	A1′
456	454	453	A2″
	504	490	A2′
	565	566	A2″
		602	A1″
700	700	701	E2″
738	735	735	E1″
		866	A1″
	1024	1009	E2′
1060	1060	1060	E2′
		1128	A2″
1180	1184	1182	A1′
1227	1227	1228	A1′
	1339	1377	E2′
1443		1444	A2′
1467	1462	1468	A1′
1510		1510	E2′
1563	1563	1563	E1″

In addition, it is found that the net-assembled Au nanoparticles are also applicable to SEIRA. Figure 6A shows the infrared absorption spectra of C_{60} on the AAO template with pyridine as the solvent media and C_{60} from the net-assembled Au nanoparticles. The small quantity of C_{60} molecules (ca. 2 mL × 0.01 M) on the AAO template presents weak infrared absorption, which is enhanced in the SEIRA from the net-assembled Au nanoparticles. Nevertheless, we did not observe the expected four infrared-active T_{1u} vibrations. Only two enhanced absorptions are observed at 1467 and 1560 cm^{-1}. The observed absorption at 1467 cm^{-1} is in good agreement with the Ag (2) pentagonal pinching vibration of C_{60} at 1468 cm^{-1}. Given the size of C_{60}, its vibrational frequencies should shift only slightly upon the formation of the Au−C_{60} complex, and

may be overlapped with the infrared-active absorptions of the C_{60} precursor.[25] A similar SEIRA spectrum is also obtained for C_{70}, as shown in Figure 6B.

It should be mentioned that no reasonable SEIRA is observable from the layer-coated Au nanoparticles. As one may know, the mechanism for SEIRA has been demonstrated with rare similarity to SERS. It has been well-documented that SERS originates primarily from two effects:[28] electromagnetic field enhancement caused by LSPR associated with metallic nanostructures and chemical enhancement caused by resonance Raman-like interaction between the metallic nanostructure and adsorbate. For SEIRA, it was reported that the attenuated total reflection (ATR) geometry in infrared absorption achieves a large effective surface area without the need for powder sample or molecular film.[28] It is likely that the adsorption of C_{60}/C_{70} on Au allows the symmetry lowering, which is beneficial not only to SERS measurement but also to the SEIRA. At the same time, the net-assembled Au nanoparticles present remarkable SPR, giving a strong local electric field, which can also bring forth contributions to the vibrational modes with either Raman-activity or infrared-activity. The synchronous observation of the SERS and SEIRA in this system indicates that the local electric field of SPR plays the dominant role for the physically adsorbed C_{60} or C_{70} molecules.

The porous nanonet of Au nanoparticles assembly on the AAO template shows infiltrative properties, which benefits the decentralization of the drops of fullerene C_{60}/C_{70} clusters on the background substrates. Recently Yu et al.[29] showed that besides the nanodisk arrays exhibiting the SERS effect, regular Au nanohole (100−600 nm) arrays fabricated via electron beam lithography also exhibit a strong SERS effect attributed to the electromagnetic coupling between the holes. Here, the fabricated nanonet of the Au nanoparticles also shows several hundred nanometer net-holes, which is assumed to give contributions to the SERS and SEIRA effect.

4. Conclusions

We extend the applications of AAO templates onto the filtration and assembly for Au nanoparticles. It is found that the colloidal Au nanoparticles can be washed cleanly and arranged into a nanonet-like array along the edge of AAO pores. Taking fullerene C_{60}/C_{70} as probe molecules and the filtrated Au nanoparticles as substrate, we obtained high-quality SERS spectra and SEIRA spectra. The synchronous observation of the SERS and SEIRA indicates that the local electric field of SPR plays the dominant role in the Raman scattering and infrared absorption for the physically adsorbed C_{60} or C_{70} molecules. Such a work is expected to be helpful for the design and development of highly active substrates for SERS and SEIRA investigation.

Acknowledgment. This work was supported by the National Natural Science Foundation of China (Nos. 50221201, 90301010, 20373077, 20471062, and 50573084) and the Chinese Academy of Sciences.

Supporting Information Available: Figures giving a sketch map illustration of the filtration methods; SEM images of the as-prepared AAO templates with 20 and 20nm pores; and Raman of only pyridine solvent media (after volatilization) on Au nanoparticles assembled on the AAO template, Raman of only C_{60} pyridine solution on the AAO template, and SERS of C_{60} from net-assembled Au nanoparticles on an AAO template. This material is available free of charge via the Internet at http://pubs.acs.org.

References and Notes

(1) (a) Ebbesen, T. W.; Lezec, H. J.; Ghaemi, H. F.; Thio, T.; Wolff, P. A. *Nature* **1998**, *391*, 667. (b) Dirix, Y.; Bastiaansen, C.; Caseri, W.; Smith, P. *Adv. Mater.* **1999**, *11*, 223.

(2) (a) Elghanian, R.; Storhoff, J. J.; Mucic, R. C.; Letsinger, R. L.; Mirkin, C. A. *Science* **1997**, *277*, 1078. (b) Henglein, A.; Meisel, D. *J. Phys. Chem. B* **1998**, *102*, 8364. (c) Haes, A. J.; Van Duyne, R. P. *J. Am. Chem. Soc.* **2002**, *124*, 10596. (d) Zhao, J.; Zhang, X.; Yonzon, C. R.; Haes, A. J.; Van Duyne, R. P. *Nanomedicine* **2006**, *1*, 219.

(3) Knoll, W. *Annu. Rev. Phys. Chem.* **1998**, *49*, 569. (b) Quinten, M.; Leitner, A.; Krenn, J. R.; Aussenegg, F. R. *Opt. Lett.* **1998**, *23*, 1331. (c) Brongersma, M. L.; Hartman, J. W.; Atwater, H. A. *Phys. Rev. B* **2000**, *62*, R16356. (d) Egusa, S.; Liau, Y. H.; Scherer, N. F. *Appl. Phys. Lett.* **2004**, *84*, 1257.

(4) (a) Freeman, R. G.; Grabar, K. C.; Allison, K. J.; Bright, R. M.; Davis, J. A.; Guthrie, A. P.; Hommer, M. B.; Jackson, M. A.; Smith, P. C.; Walter, D. G.; Natan, M. J. *Science* **1995**, *267*, 1629. (b) Kahl, M.; Voges, E.; Kostrewa, S.; Viets, C.; Hill, W. *Sens. Actuators, B* **1998**, *51*, 285. (c) McFarland, A. D.; Young, M. A.; Dieringer, J. A.; Van Duyne, R. P. *J. Phys. Chem. B* **2005**, *109*, 11279. (d) Sung, J.; Hicks, E. M.; Van Duyne, R. P.; Spears, K. G. *J. Phys. Chem. C* **2008**, *112*, 4091–4096.

(5) (a) Bohren, C. F.; Huffman, D. R. *Absorption and Scattering of Light by Small Particles*; Wiley-VCH: Weinheim Germany, 2004. (b) Haynes, C. L.; Van Duyne, R. P. *J. Phys. Chem. B* **2001**, *105*, 5599. (c) Chan, G. H.; Zhao, J.; Hicks, E. M.; Schatz, G. C.; Van Duyne, R. P. *Nano Lett.* **2007**, *7*, 1947.

(6) (a) Jensen, T. R.; Duval, M. L.; Kelly, K. L.; Lazarides, A. A.; Schatz, G. C.; Van Duyne, R. P. *J. Phys. Chem. B* **1999**, *103*, 9846. (b) Kelly, K. L.; Coronado, E.; Zhao, L.; Schatz, G. C. *J. Phys. Chem. B* **2003**, *107*, 668.

(7) (a) Enders, D.; Rupp, S.; Kuller, A.; Pucci, A. *Surf. Sci.* **2006**, *600*, L305. (b) Kosower, E. M.; Markovich, G.; Borz, G. *J. Phys. Chem. B* **2004**, *108*, 12873. (c) Bjerke, A. E.; Griffiths, P. R. *Appl. Spectrosc.* **2002**, *56*, 272A–285A. (d) Krauth, O.; Fahsold, G.; Lehmann, A. *Surf. Sci.* **1999**, *433*, 79. (e) Osawa, M.; Ikeda, M. *J. Phys. Chem.* **1991**, *95*, 9914.

(8) (a) Tamaru, H.; Kuwata, H.; Miyazaki, H. T.; Miyano, K. *Appl. Phys. Lett.* **2002**, *80*, 1826. (b) Su, K.-H.; Wei, Q.-H.; Zhang, X.; Mock, J. J.; Smith, D. R.; Schultz, S. *Nano Lett.* **2003**, *3*, 1087. (c) Rechberger, W.; Hohenau, A.; Leitner, A.; Krenn, J. R.; Lamprecht, B.; Aussenegg, F. R. *Opt. Commun.* **2003**, *220*, 137. (d) Gunnarsson, L.; Rindzevicius, T.; Prikulis, J.; Kasemo, B.; Kä ll, M.; Zou, S.; Schatz, G. C. *J. Phys. Chem. B* **2005**, *109*, 1079. (e) Atay, T.; Song, J.-H.; Nurmikko, A. V. *Nano Lett.* **2004**, *4*, 1627. (f) Jain, P. K.; Huang, W.; El-Sayed, M. A. *Nano Lett.* **2007**, *7*, 2080.

(9) Haynes, C. L.; McFarland, A. D.; Zhao, L.; Van Duyne, R. P.; Schatz, G. C.; Gunnarsson, L.; Prikulis, J.; Kasemo, B.; Kä ll, M. *J. Phys. Chem. B* **2003**, *107*, 7337.

(10) (a) Sung, J.; Hicks, E. M.; Van Duyne, R. P.; Spears, K. G. *J. Phys. Chem. C* **2007**, *111*, 10368. (b) Zou, S.; Zhao, L.; Schatz, G. C. *Proc. SPIE-Int. Soc. Opt. Eng.* **2003**, *5221*, 174. (c) Bouhelier, A.; Bachelot, R.; Im, J. S.; Wiederrecht, G. P.; Lerondel, G.; Kostcheev, S.; Royer, P. *J. Phys. Chem. B* **2005**, *109*, 3195. (d) Maier, S. A.; Kik, P. G.; Atwater, H. A. *Appl. Phys. Lett.* **2002**, *81*, 1714.

(11) Wei, Q.-H.; Su, K.-H.; Durant, S.; Zhang, X. *Nano Lett.* **2004**, *4*, 1067.

(12) (a) Whitesides, G. M.; Grzybowski, B. *Science* **2002**, *295*, 2418–2421. (b) Holtz, J. H.; Asher, S. A. *Nature* **1997**, *389*, 829–832. (c) Kobayashi, N.; Egami, C. *Opt. Lett.* **2005**, *30*, 299–301. (d) Vlasov, Y. A.; Bo, X.-Z.; Sturm, J. C.; Norris, D. J. *Nature* **2001**, *414*, 289–293.

(13) (a) Xia, D.; Brueck, S. R. J. *Nano Lett.* **2004**, *4*, 1295–1299. (b) Amos, F. F.; Morin, S. A.; Streifer, J. A.; Hamers, R. J.; Jin, S. *J. Am. Chem. Soc.* **2007**, *129*, 14296–14302. (c) Kalsin, A. M.; Fialkowski, M.; Paszewski, M.; Smoukov, S. K.; Bishop, K. J. M.; Grzybowski, B. A. *Science* **2006**, *312*, 420–424. (d) Yin, Y.; Lu, Y.; Gates, B.; Xia, Y. *J. Am. Chem. Soc.* **2001**, *123*, 8718–8729.

(14) (a) Xu, J.; Xia, J.; Lin, Z. *Angew. Chem., Int. Ed.* **2007**, *46*, 1860–1863. (b) Malaquin, L.; Kraus, T.; Schmid, H.; Delamarche, E.; Wolf, H. *Langmuir* **2007**, *23*, 11513–11521. (c) Huang, J.; Kim, F.; Tao, A. R.; Connor, S.; Yang, P. *Nat. Mater.* **2005**, *4*, 896–900. (d) Huang, J.; Tao, A. R.; Connor, S.; He, R.; Yang, P. *Nano Lett.* **2006**, *6*, 524–529. (e) Bigioni, T. P.; Lin, X.-M.; Nguyen, T. T.; Corwin, E. I.; Witten, T. A.; Jaeger, H. M. *Nat. Mater.* **2006**, *5*, 265–270. (f) Deegan, R. D.; Bakajin, O.; Dupont, T. F.; Huber, G.; Nagel, S. R.; Witten, T. A. *Nature* **1997**, *389*, 827–829. (g) Brinker, C. J.; Lu, Y.; Sellinger, A.; Fan, H. *Adv. Mater.* **1999**, *11*, 579–585.

(15) Cai, Y.; Zhang, B. M. *J. Am. Chem. Soc.* **2008**, *130*, 6076−6077.

(16) (a) Masuda, H.; Fukuda, K. *Science* **1995**, *268*, 1466. (b) Redl, F. X.; Cho, K. S.; Murray, C. B.; O'Brien, S. *Nature* **2003**, *423*, 968–971. (c) Son, D. H.; Hughes, S. M.; Yin, Y. D.; Alivisatos, A. P. *Science* **2004**, *306*, 1009–1012. (d) Harman, T. C.; Taylor, P. J.; Walsh, M. P.; LaForge, B. E. *Science* **2002**, *297*, 2229. (e) Venkatasubramanian, R.; Siivola, E.; Colpitts, T.; O'Quinn, B. *Nature* **2001**, *413*, 597. (f) Prieto, A. L.; Martın-

Gonzalez, M.; Keyani, J.; Gronsky, R.; Sands, T.; Stacy, A. M. *J. Am. Chem. Soc.* **2003**, *125*, 2388–2389.

(17) (a) Nielsch, K.; Müller, F.; Li, A. P.; Gösele, U. *Adv. Mater.* **2000**, *12* (8), 582. (b) Cui, Y.; Lieber, C. M. *Science* **2001**, *291*, 851. (c) Prieto, A. L.; Gonzalez, M. M.; Keyani, J.; Gronsky, R.; Sands, T.; Stacy, A. M. *J. Am. Chem. Soc.* **2003**, *125*, 2388. (d) Xu, D.; Xu, Y.; Chen, D.; Guo, G.; Gui, L.; Tang, Y. *Chem. Phys. Lett.* **2000**, *325*, 340. (e) Li, A. P.,; Müller, F.; Birner, A.; Nielsch, K.; Gösele, U. *Adv. Mater.* **1999**, *11* (6), 483. (f) Masuda, H.; Asoh, H.; Watanabe, M. *Adv. Mater.* **2001**, *13*, 189–191.

(18) Gasparac, R.; Kohli, P.; Mota, M. O.; Trofin, L.; Martin, C. R. *Nano lett.* **2004**, *4*, 513.

(19) Prieto, A. L.; Gonzalez, M. M.; Keyani, J.; Gronsky, R.; Sands, T.; Stacy, A. M. *J. Am. Chem. Soc.* **2003**, *125*, 2388.

(20) Lu, Q. Y.; Gao, F.; Komarneni, S.; Mallouk, T. E. *J. Am. Chem. Soc.* **2004**, *126*, 8650.

(21) Smirnov, A. I.; Poluektov, O. G. *J. Am. Chem. Soc.* **2003**, *125*, 8434.

(22) Frens, G. *Nat. Phys. Sci.* **1973**, *20*, 241.

(23) Luo, Z. X.; Liu, Y.; Kang, L.; Wang, Y.; Fu, H.; Ma, Y.; Yao, J.; Loo, B. H. *Angew. Chem., Int. Ed.* **2008**, *47*, 1–5.

(24) (a) Ganeev, R. A.; Ryasnyansky, A. I.; Kodirov, M. K.; Usmanov, T. *Opt. Commun.* **2000**, *185*, 473. (b) Li, Y.; Huang, Y.; Du, S.; Liu, R. *Chem. Phys. Lett.* **2001**, *335*, 524–532. (c) Jiang, Y. S.; Liu, C. G.; Shao, Y. H. *Prog. Phys.* **1995**, *15* (3), 307–317. (d) Gregory, K. D.; Korst, L. M.; Cane, P.; Platt, L. D.; Kahn, K.; Rafailov, P. M.; Hadjiev, V. G.; Jantoljak, H.; Thomsen, C. *Solid State Commun.* **1999**, *112*, 517–520. (e) Fagerström, J.; Stafström, S. *Phys. Rev. B* **1993**, *48*, 11367–11374.

(25) (a) Lyon, J. T.; Andrews, L. *ChemPhysChem* **2005**, *6*, 229–232. (b) Chase, S. J.; Bacsa, W. S.; Mitch, M. G.; Pilione, L. J.; Lannin, J. S. *Phys. Rev. B* **1992**, *46*, 7873.

(26) (a) Schettino, V.; Pagliai, M.; Ciabini, L.; Cardini, G. *J. Phys. Chem. A* **2001**, *105*, 11192–11196. (b) Choi, C. H.; Kertesz, M.; Mihaly, L. *J. Phys. Chem. A* **2000**, *104*, 102. (c) Menéndez, J.; Page, J. B. Light Scattering in Solids. In *Topics in Applied Physics*; Cordona, M., Güntherodt, G., Eds.; Springer-Verlag: Berlin, Germany, 2000; p 27.

(27) (a) Luo, Z. X.; Fang, Y. *Chem. Phys.* **2006**, *321*, 86. (b) Luo, Z. X.; Fang, Y. *Vibra. Spectrosc.* **2005**, *39*, 151. (c) Luo, Z. X.; Fang, Y. *J. Colloid Interface Sci.* **2006**, *301*, 184. (d) Yang, X. C.; Fang, Y. *J. Phys. Chem. B* **2003**, *107*, 10100–10103. (e) Fang, Y.; Huang, Q.-J.; Wang, P.; Li, X. Y.; Yu, N. T. *Chem. Phys. Lett.* **2003**, *381*, 255.

(28) (a) Moskovits, M. *Rev. Mod. Phys.* **1985**, *57*, 783. (b) Furtak, T. E.; Roy, D. *Surf. Sci.* **1985**, *158*, 126–146. (c) Guo, W.; Zhang, P. *Chin. J. Chem. Phys.* **1989**, *2*, 168–176. (d) Pan, D.; Ma, Y. *Acta Phys. Sinica* **1995**, *44*, 1914–1920.

(29) Yu, Q.; Guan, P.; Qin, D.; Golden, G.; Wallace, P. M. *Nano lett.* **2008**, *8*, 1923–1928.

JP810387W